ADVANCES IN X-RAY DIFFRACTOMETRY OF CLAY MINERALS

by

WILLIAM PARRISH

Philips Laboratories, Irvington-on-Hudson, New York

ABSTRACT

The introduction of counter tubes and the related instrument geometries have made it possible to obtain greatly improved x-ray powder patterns. Most of the important factors that must be understood in x-ray diffractometry are described in terms of their effect on the intensity, peak-to-background ratio, resolution and line shape. These factors are the geometry of the x-ray optical system, the x-ray tube focal spot size, the angular apertures of the primary beam in the focusing and axial planes, the 2 : 1 setting, and the receiving slit. The precision is often limited by the specimen preparation rather than the instrument, and the effects of homogeneity, displacement and transparency, crystallite sizes, and preferred orientation are outlined. A new diffractometer arrangement employing a transmission specimen followed by a focusing crystal monochromator is shown to be a useful supplement to the standard reflecting specimen diffractometer for clay mineral studies. The important characteristics of Geiger, proportional and scintillation counters are described in terms of linearity, quantum counting efficiency, pulse amplitude distribution and counting statistics. A bibliography of key literature references is appended.

INTRODUCTION

X-ray diffraction is now an accepted physical method for investigating clay minerals and is often used with other physical methods such as electron diffraction, electron microscopy, differential thermal analysis, and petrographic examination for crystallographic and phase studies. In recent years the x-ray method has been greatly improved by introduction of counter tubes which have largely supplanted film methods. Although the counter tube method can provide superior data, the full potential of the method is not frequently realized for a variety of reasons. Many papers have been published on the results obtained with the counter tube diffractometer (see for example *American Mineralogist*, *American Journal of Science*, *Journal of the American Ceramic Society*, etc.) but very little has appeared on the theory and technique of the method. The purpose of this paper is to present some of the more important practical factors of powder diffractometry in non-mathematical form so that the clay mineral analyst can use the method to its fullest potential and with greater confidence. It is not possible to present a detailed discussion, and instead references to key papers will be given.

There are two general categories of x-ray studies of clay minerals. By far the most widespread applications of the method are for identification, phase analysis, and the like. In some cases the x-ray powder patterns are used as

https://doi.org/10.1346/CCMN.1958.0070115 Published online by Cambridge University Press

an aid in stratigraphic correlation and thousands of patterns are required more or less on a production basis. The other category is confined to relatively few laboratories and includes the study of distorted crystals, faulty or mistake structures of various types, small crystallite size line broadening, strain and similar properties (see for example, Warren, 1959; Wilson, 1949). In the earlier x-ray studies of these latter phenomena it was not possible to obtain precise quantitative data on the line profiles, and aside from a quali-

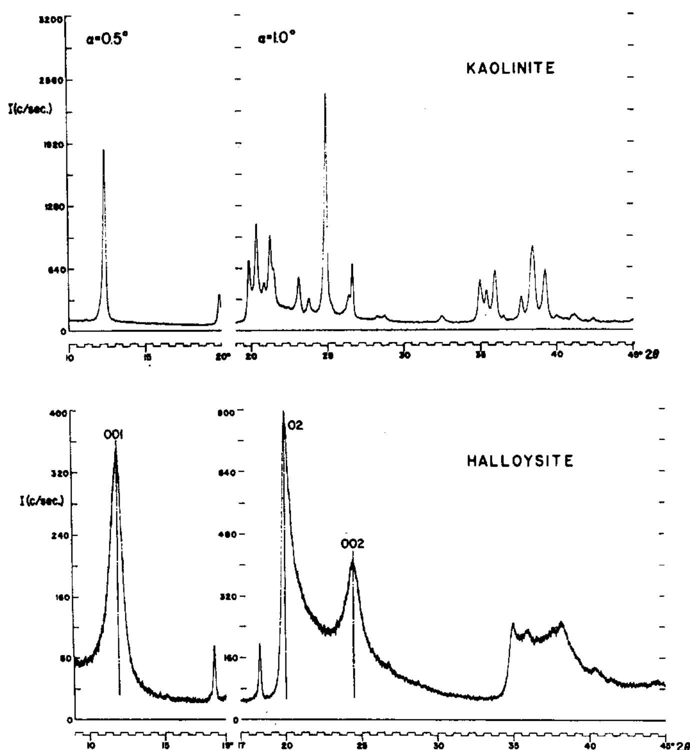

FIGURE 1.—Diffractometer recordings of kaolinite (above), Mesa Alta, New Mexico (A.P.I. Project 49, no. H–9) and halloysite (below), Bedford, Indiana (A.P.I. Project 49, no. H–12). Dry, stationary, reflecting specimens. CuK 40 kVp (above), 35 kVp (below), 20 mA, 0.0007 in. Ni filter, scintillation counter with discrimination, receiving slit 0.075°, scan speed $\frac{1}{4}$°/min, time constant 4 sec, $\alpha = 0.5°$ for small angle region, $\alpha = 1°$ for high angle region.

tative description including perhaps the line breadth, relatively little detailed information could be obtained on the complex features of the structure. With modern diffractometers (Parrish and Hamacher, 1952; Parrish, Hamacher and Lowitzsch, 1954–1955) it is possible to observe small but significant differences in line profiles, such as details of the entire line shape and asymmetry, the form of the tails, and shifts of the peak or centroid, so that Fourier analysis is feasible. In addition, considerable progress is being made on the

https://doi.org/10.1346/CCMN.1958.0070115 Published online by Cambridge University Press

development of counter methods for single structure analysis so that many problems that could not be handled in the past may be re-examined with these new, more powerful tools.

Clay mineral powder patterns commonly are characterized by many overlapping lines resulting from their low symmetry, low-intensity lines particularly at the higher angles where they may be difficult to distinguish from the background, low-angle lines from the large *d*-spacings, strong preferred orientation, broadened line profiles resulting from small crystallite sizes, lines with different background levels on either side, asymmetric lines from " mistake " structures, " bands " of reflections and other unusual features not often found in well-crystallized substances. Fig. 1 shows diffractometer recordings of kaolinite and halloysite with many of these characteristics. These recordings show better relative intensities and line shapes, lower background, and higher peak-to-background ratio and resolution than previously published film data (compare for example with Kerr *et al.*, 1950; Brindley, 1951).

Although the present review is directed specifically toward powder diffractometry, most of the principles to be discussed are equally applicable to x-ray spectrochemical analysis by means of fluorescence, which recently has been developed for elemental analysis and has proved to be a valuable supplement to diffraction analysis (Parrish, 1955–1956b; Mack, 1956). It is used for qualitative and quantitative analysis of all elements of atomic number above about 12 or 13. The elements in the lower atomic number range 12 to 24 require a vacuum or helium path. The reader may refer to recent volumes of *Analytical Chemistry* for the many types of analyses that are possible with this method.

ACKNOWLEDGMENT

The writer is indebted to Dr. P. H. Dowling and Mrs. J. Taylor of this Laboratory for critically reviewing the manuscript.

DIFFRACTOMETER GEOMETRY

The interpretation of such complicated patterns shown in Fig. 1 may be subject to considerable error unless the instrumental factors are clearly understood. In analyzing a line profile, for example, it is necessary to know what portion of the asymmetry is caused by the instrument so that it can be subtracted (i.e. unfolded) from the observed profile to obtain the pure diffraction effects of the specimen. In the following sections the more important aspects of the instrument geometry will be described.

X-ray Optical System

The x-ray optical system of modern powder diffractometers is shown in Fig. 2 (Parrish, 1949). The goniometer axis of rotation O lies at a distance R, the goniometer radius, from the source and from the receiving slit. A relatively large reflecting specimen, about 10×20 mm, is rotated automatically

https://doi.org/10.1346/CCMN.1958.0070115 Published online by Cambridge University Press

at one-half the angular speed of the goniometer arm which carries the receiving slit and counter tube, to maintain the correct focusing conditions at all reflection angles. The narrow source *F* and receiving slit *RS* are required to obtain high resolution. The parallel or Soller slits SS_1 and SS_2 limit the divergence of the beam in the plane normal to the focusing plane. They make it possible to use an extended source to obtain high intensities with a minimal deterioration of the line shape. The scanning plane of the goniometer may be horizontal (e.g. General Electric) or vertical (e.g. Philips).

The divergent primary beam is diffracted by the specimen and converges at the receiving slit. This " focusing " action is not perfect because of the use of a flat specimen rather than one with a continuously changing curvature, penetration of the beam into the specimen, instrumental aberrations, the

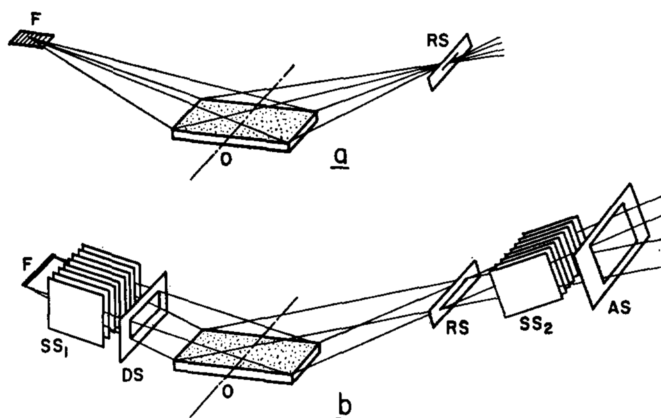

FIGURE 2.—x-ray optical systems of diffractometer. (a) Previous low resolution system using spot source, (b) present high resolution system with narrow line source. *F* focal spot of x-ray tube, *O* goniometer axis of rotation, *DS* divergence slit, *RS* receiving slit, *AS* anti-scatter slit, SS_1 and SS_2 Soller slit assemblies (*Philips Tech. Rev.*, v. 16, 1954).

finite size and wave-length distribution of the source, and similar factors. Consequently the lines are displaced slightly from their correct positions and the profiles are slightly distorted. These distortions are usually smaller than those occurring in Debye–Scherrer cameras, and moreover have been analyzed extensively so that allowances can be made for them. The upper limit of the counter tube scanning range is about 165° 2 θ because of mechanical interference of the counter tube with the x-ray tube housing. It is possible to scan down to about 1° or less if the instrument is properly aligned.

The use of anti-scatter slits reduces the x-ray background. The slit *AS* placed behind the receiving slit in Fig. 2 limits the aperture of the counter tube to the irradiated area of the specimen. A cylindrical slot in the radiation protection shield around the specimen (not shown in Fig. 2) prevents the primary beam from striking the sides of the specimen holder along the *O*-

https://doi.org/10.1346/CCMN.1958.0070115 Published online by Cambridge University Press

direction. One of the inherent advantages of the counter tube method is that the background is always lower than that of film. The specimen scatters the primary beam at all angles and thus continually builds up the background over the entire film during the exposure. In the counter method the anti-scatter slits limit the scattered background, which is recorded point by point. Electronic discrimination (see below) also limits the spectral range of the recorded background, thereby greatly increasing the peak-to-background ratio.

One of the most common sources of difficulty arises in the alignment and angular calibration of the instrument. If these are not properly carried out it becomes impossible to compare results obtained at different laboratories or even in the same laboratory. The alignment, the proper selection of slit sizes, and the counter tube technique have a profound effect on the intensity, peak-to-background ratio, and resolution, which are the principal factors determining the quality of the x-ray pattern, and hence the information that can be obtained from it. A simple mechanical method for alignment, determination of the 0° angle without calibration standards and the 2 : 1 setting is described in detail in a recent article (Parrish and Lowitzsch, 1959), and the other factors will be described below.

X-ray Tube Focus

The focal line of the x-ray tube generally is used as the geometrical source of the x-ray optical system. The dimensions of the line are usually 1–1.6 mm by 10–15 mm in commercial sealed-off diffraction tubes. The focal line is viewed at a small grazing angle ψ of 3°–6° to the target surface. In earlier diffractometers (Lindemann and Trost, 1940; Friedman, 1945) the long axis of the focal line was oriented normal to O, giving a nearly square source; while in present-day instruments it is parallel to O, giving a long narrow line source (Fig. 2). The effective width of the source, i.e. the projected dimension in the direction normal to O, adds a symmetrical broadening to each line, and hence has a considerable effect on the resolution of the instrument. The width of the CuKα_1 line of a partially resolved doublet in the front-reflection region is about 0.10° 2 θ wide at one-half peak height when a well-crystallized specimen is used on a modern diffractometer set up for good resolution, while the older instruments gave a line breadth three or four times greater under comparable conditions. The dispersion increases rapidly in the back-reflection region, and hence the recorded line breadths also increase with reflection angle because of the spectral width of the x-ray emission lines.

With increasing ψ the intensity of the radiation from the focal line rises rapidly from zero at $\psi = 0°$ at a rate dependent on the x-ray tube voltage, the atomic number of the target element, the smoothness of the target surface and similar factors. The x-ray tube window subtends an angle of about 9° at the focal line, and the angular aperture of the primary beam in the focusing plane, i.e. the plane normal to O, may be as large as 4° in the back-reflection region. The larger the ψ-angle, the greater the intensity and the projected

https://doi.org/10.1346/CCMN.1958.0070115 Published online by Cambridge University Press

width. The broadening caused by the source width is symmetrical and the same at all reflection angles. Other instrumental aberrations, however, contribute to the line width and mask the effect of the variation of the intensity of the source. In practice, increasing the ψ-angle from 3° to 6° gives about 25 percent greater intensity with no loss of resolution, but the maximum scanning angle is then reduced to 162° 2 θ. Alternatively, ψ may be left at 3° but the width of the focus increased by a factor of 2 in the manufacture of the tube, and hence the intensity doubled without increasing the specific loading of the target. If both the larger source and ψ-angle are used, the intensity is increased by a factor of more than 2 and there is only a small loss of resolution (Parrish, 1958). The line profiles in Fig. 3 illustrate these effects.

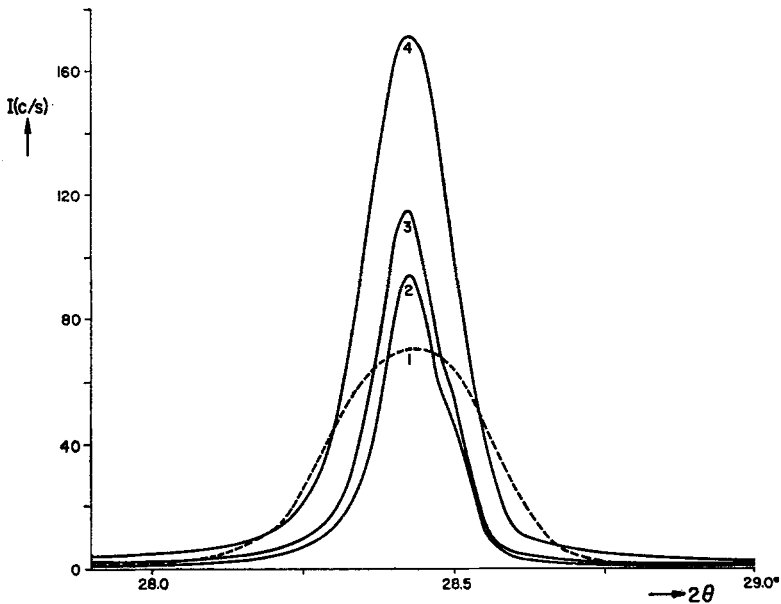

FIGURE 3.—Effect of source size on line profiles : 111 reflection of silicon powder with CuKα radiation $\alpha = 1°$, receiving slit = 0.05°.

No.	Source	Actual Size (mm)	ψ	Projected Size (mm)
1	Spot	1.6 × 10	6°	1.6 × 1.0
2	Line	1.6 × 10	3°	0.08 × 10
3	Line	1.6 × 10	6°	0.16 × 10
4	Line	3.2 × 12	6°	0.32 × 12

Angular Aperture in the Focusing Plane

The angular aperture α of the divergent beam in the focusing plane is determined by the width of the divergence slit. The irradiated specimen length l varies with glancing angle θ according to the approximate relationship $l = \alpha R/\sin\,\theta$ (α in radians), and l thus increases rapidly at the small

https://doi.org/10.1346/CCMN.1958.0070115 Published online by Cambridge University Press

angles. This sets a lower limit to the angles that should be measured with a given aperture and specimen length. If scanning is continued below this minimum angle, scattering from the ends of the specimen holder may cause an increase in the background; also it will not be possible to relate directly the intensities of the lines above and below the angle at which l exceeds the actual specimen length. If scanning is continued far below this minimum angle, the upper portion of the direct beam may pass over the top of the specimen and enter the counter tube. Since the intensity increases with α, it is generally desirable to change the divergence slit a few times when scanning over a wide angular range, always using the largest possible α. Whenever α is changed the relative intensities may be measured by overlapping a small region with both apertures, as shown in Fig. 1. Table 1 lists

TABLE 1.—DATA FOR DIVERGENCE SLIT IN FOCUSING PLANE[1]

Angular Aperture α	$2\theta_{min}$	Maximum d-spacing (Å)		
		MoKα	CuKα	CrKα
5′	1.45°	28	62	92
30′	8.50	4.8	10.4	15.5
1°	17.0	2.4	5.2	7.8
2°	34.5	1.2	2.6	3.9
4°	72.8	0.6	1.3	1.9

[1] For R = 170 mm, l = 20 mm.

the minimum 2θ angle and the corresponding maximum d-spacing that may be obtained with MoKα, CuKα and CrKα radiations with several apertures for the case $l = 20$ mm, $R = 170$ mm.

It has also been suggested (de Wolff, 1957) that the aperture be changed synchronously with reflection angle so that the entire specimen length is always illuminated. This would require some modifications to the usual simple methods of measuring relative intensities but would have the advantage of the maximum intensity at all reflection angles.

Ideally the specimen should be curved to fit the focusing circle whose radius of curvature $r = R/2 \sin \theta$. The curvature of the specimen surface thus would be required to change continually during scanning, and because this is usually impractical, a flat specimen is used as shown in Fig. 4. The primary rays striking the specimen do not all make the same θ-angle with the surface, and hence the focusing is imperfect. Consequently the recorded diffracted profile is asymmetrically broadened and shifted toward smaller angles (Wilson, 1950). In routine work no corrections are normally made for this flat-specimen aberration, but in precision measurements and analyses of the line profiles corrections may be required (Parrish and Wilson, 1959). The effect may be reduced by decreasing α. It is shown in Fig. 5(a) for the

https://doi.org/10.1346/CCMN.1958.0070115 Published online by Cambridge University Press

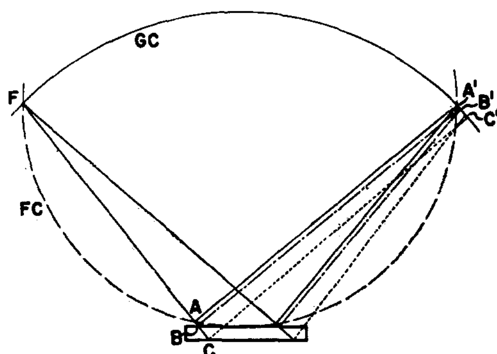

FIGURE 4.—Schematic drawing of focusing plane showing origin of flat specimen and specimen transparency errors. If the specimen were curved to fit the focusing circle *FC*, the divergent rays from the focal spot *F* would converge at *A'*. When the flat specimen is used, the line is asymmetrically broadened and shifted to smaller angles *B'*. If the rays penetrate into the specimen, a similar effect occurs, as shown by the shift to *C'*. *GC* is the goniometer circle. Displacing the specimen from *FC* shifts the line to higher or smaller angles depending on the direction of the displacement but does not broaden the line.

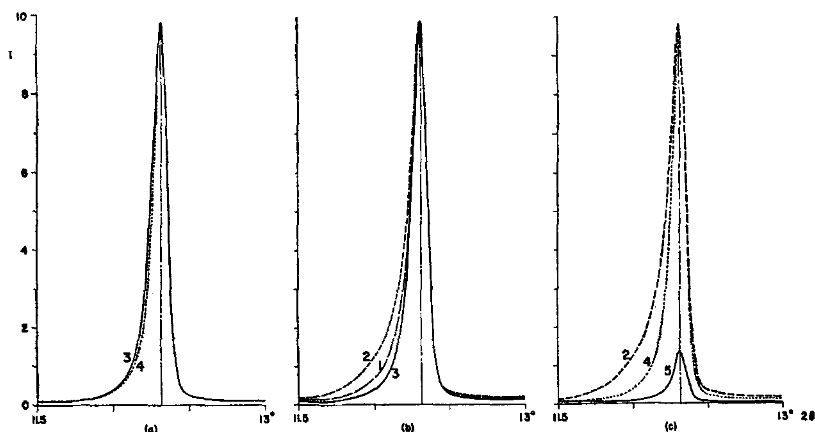

FIGURE 5.—Effect of flat specimen and axial divergence aberrations on line shape and intensity. Dickite (7 Å), CuKα, standard divergence Soller assembly, scintillation counter with discrimination, receiving slit 0.05°.

No.	α	S[1] (in.)	kVp	mA	Scale Factor
1	0.5°	0.020	40	20	64
2	0.5	None	40	13.6	64
3	0.5	0.010	40	17.5	32
4	0.17	0.010	42	24	16
5	0.17	0.010	40	13.6	64

[1] Receiving Soller slit assembly with $L = 0.5$ in.

https://doi.org/10.1346/CCMN.1958.0070115 Published online by Cambridge University Press

7 Å reflection of dickite. The experimental conditions for both profiles were identical except that profile 3 was obtained with $\alpha = 0.5°$ ($l = 14$ mm), 4 with $\alpha = 0.17°$ ($l = 4.8$ mm), and the x-ray tube current adjusted so that both profiles had the same peak intensity in order that the effect on line shape could be better seen.

Axial Divergence

The angular divergence of the primary beam in the plane normal to the focusing plane, i.e. parallel to O, is limited by the parallel slit assemblies. One set is placed between the x-ray tube and the specimen in order to limit the divergence of the primary beam, and another set is placed behind the receiving slit in order to limit the diffracted beam as shown in Fig. 2. The angular aperture δ of the beam in this plane is determined by the length L and spacing s of the thin metal foils, $\delta = 2 \tan^{-1} s/L$. The aperture δ is of the order of 4.5° for each set, and each set reduces the intensity by a factor of about 2. The axial divergence causes an asymmetric broadening of the line profile and a shift of the line toward lower angles in the front-reflection region and toward higher angles in the back-reflection region. The effect is greatest at very small angles ($<20°\ 2\theta$) and at very large angles ($>160°\ 2\theta$) and is smallest in the region from 90° to 120°. Procedures for correcting the data for axial divergence have been published (Pike, 1957).

The profiles in Fig. 5(b) show the effect of axial divergence on the 7 Å reflection of dickite. The experimental conditions were the same for the three profiles, and δ of the divergence Soller assembly was always 4.5°. The δ of the receiving Soller slit assembly was varied without disturbing the receiving slit. Line 1 was obtained with the standard assembly $L = 0.5$ in., $s = 0.020$ in., $\delta = 4.5°$; line 2 with all foils removed, $\delta =$ about 6.5°; line 3 with $L = 0.5$ in. and $s = 0.010$ in., $\delta = 2.25°$. The x-ray tube current was adjusted so that the profiles had the same peak intensities.

In the front-reflection region the high-angle side of the profiles remains unchanged and the low-angle side is shifted by both the flat-specimen and axial divergence aberrations. Consequently, the centroid of the line (center of gravity or first moment) (Ladell, Parrish and Taylor, 1959; Pike and Wilson, 1959) is shifted more than the peak. The peak shift is too small to be seen on charts of this scale. Both aberrations are shown in Fig. 5(c) where profiles 2 and 4 may be compared with the same peak intensity to see the effect on the shapes, and 2 and 5 compared to see the effect on the intensity. Profile 4 (and 5) has the greater symmetry and shorter tail, but the peak intensity has been reduced by a factor of about 8 to achieve this.

2 : 1 Setting

To obtain proper focusing conditions it is necessary that the middle of the receiving slit be at the correct 2θ-angle when the specimen surface is at θ. This 2 : 1 angular relationship must be set and then maintained by the goniometer at all reflection angles. An incorrect 2 : 1 setting causes a large decrease in peak intensity, a large increase in line breadth and asymmetry,

https://doi.org/10.1346/CCMN.1958.0070115 Published online by Cambridge University Press

and a shift of the peak toward higher angles (Fig. 6). A clockwise mis-setting causes a greater change in the line profile than a counterclockwise mis-setting. The effect decreases with increasing θ and hence may cause systematic errors in the intensity and angle measurements. The integrated line intensity

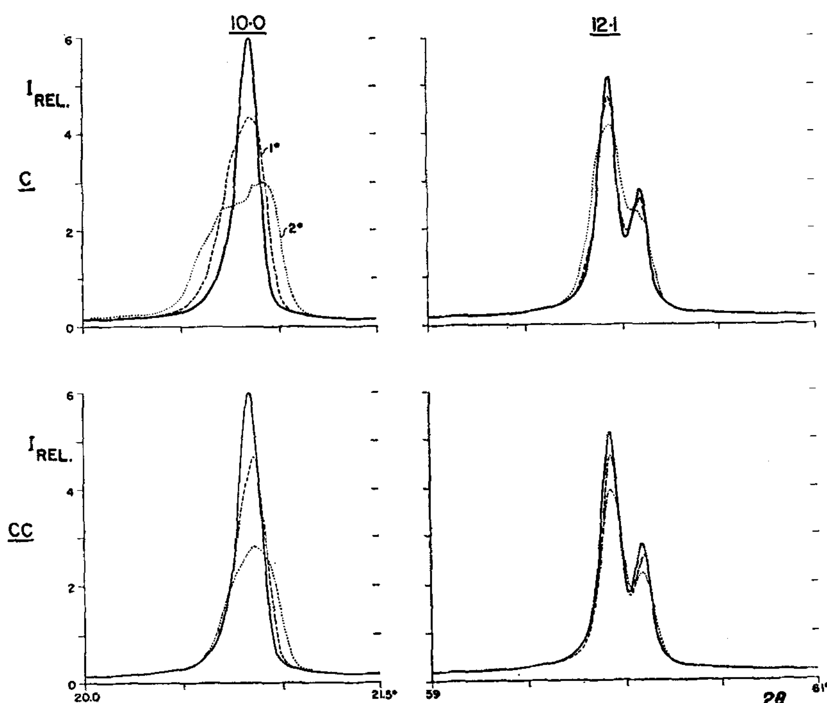

FIGURE 6.—Effect of 2 : 1 setting on line profiles of powder specimen of quartz (10·0, left), (12·1, right) with a clockwise mis-setting (above) and counterclockwise mis-setting (below). The solid line profiles were obtained with the correct 2 : 1 settings and the others with 1° and 2° mis-settings. CuKα, a = 1°, receiving slit 0.05°.

also changes in a somewhat unpredictable manner. For example, the integrated intensity measurements (normalized for highest = 100 percent) of the 10·0 quartz line shown in Fig. 6 were:

2 : 1	Integ. Int.
Correct	89%
1°C	100
2°C	99
1°CC	87
2°CC	74

https://doi.org/10.1346/CCMN.1958.0070115 Published online by Cambridge University Press

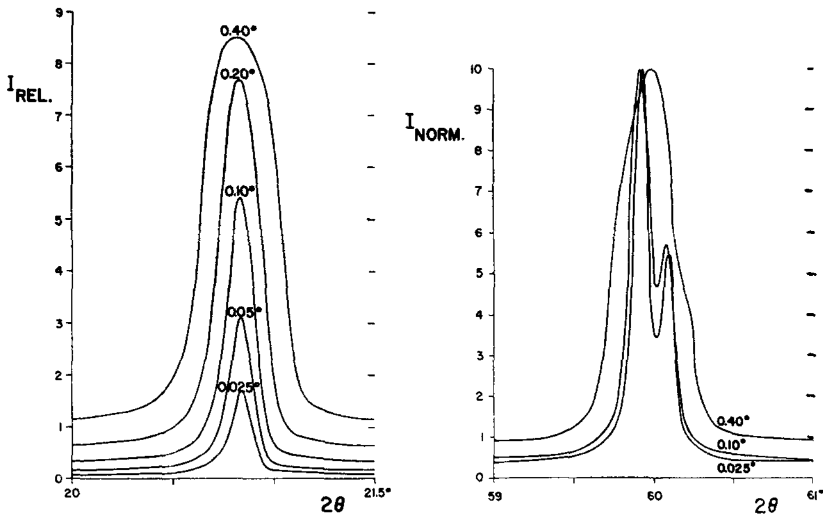

FIGURE 7.—Effect of receiving slit width on line profiles of quartz. (a) 10·0 line, tracings from original recordings. (b) 12·1 line with peak intensities normalized to same values. The receiving slit widths are given in °2θ.

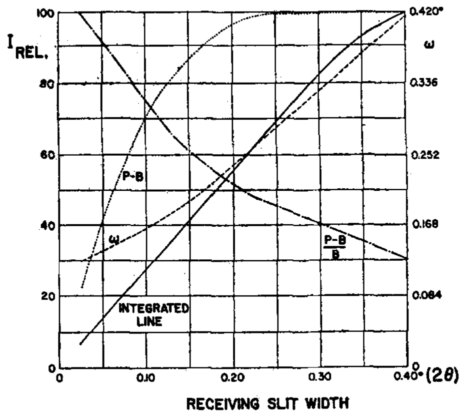

FIGURE 8.—Integrated line intensity, peak intensity P–B, peak-to-background ratio $(P$–$B)/B$ and line breadth measured at 0.5 $(P$–$B)$ as a function of receiving slit width for the 10·0 reflection of quartz.

https://doi.org/10.1346/CCMN.1958.0070115 Published online by Cambridge University Press

It is clear that the 2 : 1 setting may be the source of considerable errors and must be checked. A mechanical method for precisely setting the 2 : 1 setting has been described (Parrish and Lowitzsch, 1959).

Receiving Slit

The receiving slit width is a major factor in determining the line profiles of well-crystallized substances. Increasing the width increases the integrated line intensity and the peak intensity $P - B$, but causes a decrease in the peak-to-background ratio $(P - B)/B$ (Parrish, 1955–1956a). The receiving slit width adds a symmetrical broadening to the line and the amount of broadening is independent of diffraction angle. The line breadth ω measured at one-half peak height above background also increases with receiving slit width. When the Kα-doublet is unresolved, the angular position of the peak remains unchanged as shown in Fig. 7(a) for the 10·0 reflection of a quartz powder specimen. These effects are summarized in Fig. 8. When the receiving slit width is increased by a factor of 10 from 0.025° to 0.25°, $P - B$ has reached its maximum value and has increased by a factor of 4, $(P - B)/B$ has decreased by more than a factor of 2 and ω has increased by more than a factor of 2. When the Kα-doublet is partially resolved, the line shape changes markedly and the peak position may be shifted to higher angles, i.e. toward the centroid of the doublet, as shown in Fig. 7(b) for the 12·1 reflection. It is apparent that the intensity can be gained only at a loss of resolution and peak-to-background ratio ; therefore each problem must be analyzed to determine the more important factors and the best compromise for that particular analysis.

SPECIMEN FACTORS

Many modern diffractometers have been improved to the point that the limiting factor in the precision of the data usually is the specimen preparation rather than the instrumentation. Unfortunately, it frequently happens that too little time is spent on this important part of the x-ray analysis and the resulting errors may cause considerable confusion. Some of the problems that arise in specimen preparation are outlined below, and it is evident that much more work is required to develop better methods.

Homogeneity

The total intensity of the primary x-ray beam is constant, but the length of specimen irradiated varies with θ, and thus the brightness of the irradiated specimen area is constantly changing. Consequently, unless the specimen is perfectly homogeneous, the relative intensities of the lines cannot be compared. The specimen absorption coefficients of clay minerals usually are large enough so that only a very thin layer of the specimen surface contributes to the diffraction, and therefore it is essential that the top surface be representative of the bulk sample.

https://doi.org/10.1346/CCMN.1958.0070115 Published online by Cambridge University Press

Displacement and Transparency

If the surface of the specimen is not coincident with the goniometer axis of rotation, the observed line will be shifted from its correct angular position (Wilson, 1950; Parrish and Lowitzsch, 1959). If the specimen is displaced a distance $x_{s.d.}$ from O, the reflection is shifted $x_{s.d.}$ cos θ/R (radians). For example, if $x_{s.d.} = 0.075$ mm, a line at 20° 2 θ will be shifted 0.05° 2 θ from its correct value. The shift is toward higher angles if the specimen surface is inside the focusing circle and toward lower angles if it is outside, but the line shape is not changed if $x_{s.d.}$ is relatively small. This is one of the com-

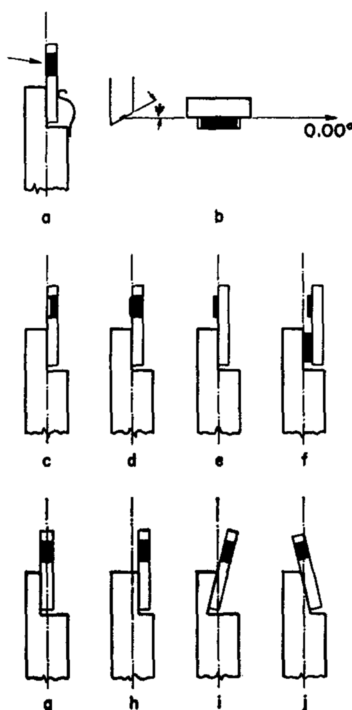

FIGURE 9.—Some examples of specimen displacement errors: (a) and (b) correct specimen and goniometer reference surface, (c) concave, and (d) convex filling of specimen holder, (e) slide coating not shimmed back, (f) slide coating shimmed back too far, (g)–(j) incorrect goniometer reference surfaces.

monest and largest of the systematic errors in diffractometry, being maximum at small angles and zero at 180°. The displacement may be caused by incorrect specimen preparation. For example, in filling the specimen holder the surface may be too low or too high (Fig. 9(c) and (d)), or in the case of a slide coating, the specimen is not shimmed back (Fig. 9(e)) or shimmed back an incorrect amount (Fig. 9(f)). It is also essential that the specimen holder be flat. If the specimen reference surface on the goniometer is not coincident with O (Fig. 9(g) to (j)), the readings will be in error by a constant amount

https://doi.org/10.1346/CCMN.1958.0070115 Published online by Cambridge University Press

at a given reflection angle regardless of whether the specimen is prepared properly or not.

Unlike the Debye–Scherrer case, where it is necessary to use specimens with low absorption to avoid line shifts, a high-absorption specimen is desirable in powder diffractometry. When the primary beam penetrates into the specimen (Fig. 4) it will be diffracted from various depths, thus causing a shift of the line from its correct position and an asymmetric broadening toward smaller angles by an amount depending upon the absorption coefficient, specimen thickness, and diffraction angle (Wilson, 1950; Keating and Warren, 1952; Parrish and Wilson, 1959). The effect is maximum at 90° 2 θ and zero at 0° and 180°. If the beam passes through the specimen the relative intensities will also be modified because the effective scattering volume will then vary with diffraction angle (Milberg, 1958). For specimens with very low absorption coefficients, it is usually desirable to prepare thin slide smears in order to avoid deterioration of the line profiles. The mounting

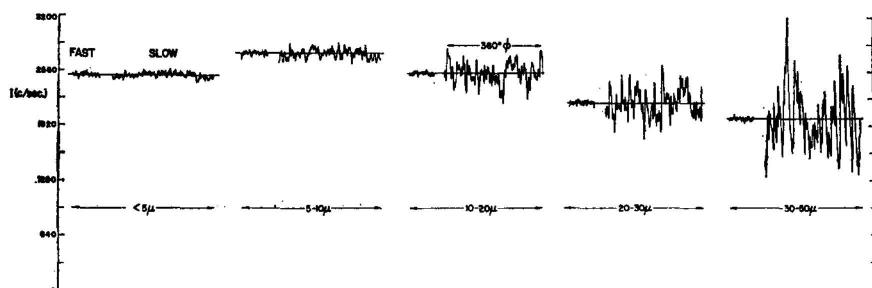

FIGURE 10.—Fast (77 rev/min) and slow ($\frac{1}{7}$ rev/min) rotation of various crystallite size specimens of silicon powder, 111 reflection, with goniometer stationary. CuKα 25 kVp, 10 mA, α = 1°, receiving slit 0.10°, time constant 2 sec.

should be on low-reflecting substrates such as properly oriented quartz single crystals (Buerger and Kennedy, 1958) or cellophane.

Crystallite Sizes

When the crystallites are very small, say $<1\mu$, the lines broaden by an amount dependent on the crystallite size and the diffraction angle, and the x-ray method is commonly used, often in conjunction with the electron or optical microscope, for crystallite size analysis. When the crystallites are large, say $>5\mu$, they have a large effect on the relative and absolute intensities as shown in Fig. 10. Rotating specimens (Parrish, 1955–1956a) were prepared from silicon powder that had been separated into several size fractions by air elutriation. The goniometer was set to receive the 111 reflection with CuKα radiation. The specimen was rotated rapidly (77 rev/min) and then slowly ($\frac{1}{7}$ rev/min) in its own plane. The rapid rotation gives an average intensity whose fluctuations are dependent only on the counting statistics (see below), and the slow rotation shows the fluctuation

https://doi.org/10.1346/CCMN.1958.0070115 Published online by Cambridge University Press

of intensity caused by the variation of the number of diffracting crystallites during rotation. When the sizes are $<5\mu$ there is no significant difference between fast and slow rotation, but as the sizes increase, the slow rotation pattern shows increasing amounts of fluctuations from the average intensity. The slow rotation patterns repeat every 360° of rotation.

The reason for these fluctuations is that not all the crystallites in the specimen are oriented to reflect. In fact, the number of crystallites properly oriented is $kN^{\frac{1}{3}}$ where k is a constant determined by the experimental conditions and is usually a small fraction of 1, and N is the number of crystallites in the specimen. Consequently only a small fraction of the crystallites have the correct orientation and the intensity varies accordingly. The relative r.m.s. deviation of the intensity is dependent on the goniometer radius, the diffraction angle, the length of the focal spot and receiving slit, the multiplicity factor of the particular reflection, and the *effective* number of irradiated crystallites. Using experimental conditions commonly applied in practice, the r.m.s. deviation improved by a factor of 8 for peak intensities and by a factor of 5 for integrated line intensities when the silicon specimen of the 30–50μ crystallites was rapidly rotated (de Wolff, Taylor and Parrish, 1959).

Measurements were also made of a 30–50μ fraction specimen of silicon, set at ten different stationary ϕ-angles selected randomly. The $111\alpha_{1+2}$ and $220\alpha_1$ lines were scanned using the same ϕ-angle for both, at $\frac{1}{4}$°/min, 4 sec time constant and the peak intensities read from the chart. The intensities for $111\alpha_{1+2}$ ranged from 1345 to 3330 c/sec and those of $220\alpha_1$ from 956 to 1504 c/sec. The ratios varied from 1.11 to 2.48. When the same specimen was rotated rapidly, the values were $111\alpha_{1+2} = 2145$, $220\alpha_1 = 1088$, ratio = 1.97. Thus if stationary specimens of large crystallite sizes are used it is apparent that there can be large errors in the intensities because there is no correlation between the azimuthal ϕ-angle at which a large intensity occurs for one line and the intensity obtained at the same ϕ-angle for another line. If stationary specimens must be used, the crystallites should be 1–5μ to obtain a 1 percent precision in the intensity measurement (Alexander, Klug and Kummer, 1948).

Rotating the specimen has little effect on the average absolute intensity. The 5–10μ fraction in Fig. 10 had the highest average intensity. The larger crystallite sizes had a lower intensity due to extinction and lower packing density. The $<5\mu$ fraction had a lower intensity due to a layer of amorphous silica around the grains, and when it was removed by selective etching the intensity increased.

The slowly rotating specimen method may be used as a crude measure of the crystallite sizes if properly calibrated. It is thus similar to the spottiness of Debye–Scherrer rings in the camera method that occurs when the specimen is not rotated.

Preferred Orientation

The completely random orientation which is assumed in powder diffractometry rarely occurs in clay minerals because of their morphology. Rotating

https://doi.org/10.1346/CCMN.1958.0070115 Published online by Cambridge University Press

the specimen reduces the second-order preferred orientation within the specimen plane but has little effect on the orientations parallel to the plane. By comparing reflection and transmission (see below) powder patterns of the *same* specimen preparation to see whether the relative intensities are the same, the degree of preferred orientation can be determined. The basal

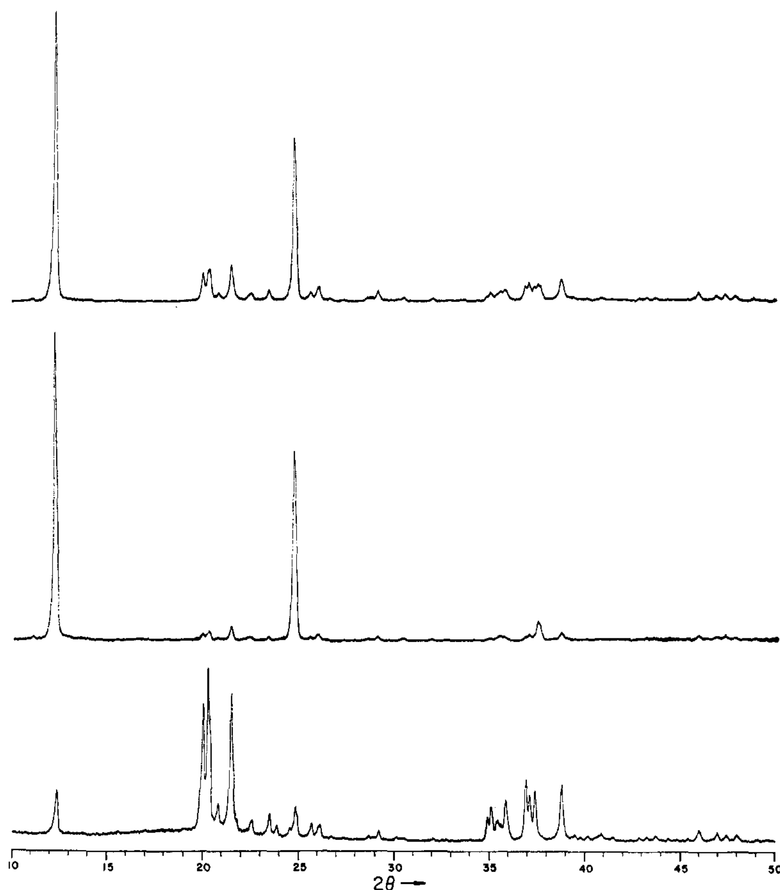

FIGURE 11.—Effect of preferred orientation on x-ray patterns of dickite. (*Top*)—thin specimen in reflection ; (*middle*)—thick reflection specimen mixed with 75 percent by volume of flour ; (*bottom*)—same specimen as used for top recording with specimen in transmission followed by focusing monochromator as shown in Fig. 12.

reflections are enhanced in reflection and reduced in transmission while the opposite occurs with the prism and pinacoid reflections. This is shown in Fig. 11 for a thin layer of dickite sprinkled on a thin sheet of cellophane coated with Vaseline. The top recording is the reflection pattern. The middle recording was made from a thick specimen mixed with 75 percent by volume of flour to try to reduce the preferred orientation, and it is apparent this

https://doi.org/10.1346/CCMN.1958.0070115 Published online by Cambridge University Press

procedure was not successful. The bottom transmission pattern was made on the same preparation as the top recording and the large differences between the two patterns are caused by the effects mentioned above.

Many methods of reducing preferred orientation have been suggested. For example, McCreery (1949) attempts to avoid the effect in packing the powder into the holder, Smallman (1952) advises the use of a side-loading specimen holder, Flörke and Saalfeld (1955) mix the powder with a plastic to coat the particles, and Porrenga (1958) cuts a saw-tooth pattern on the surface. These and other methods may be tried. One of the important advantages of using both the reflection and transmission method is that the specimen preparation may be changed and one may see almost immediately the degree of preferred orientation that still exists.

In some special cases it may be desirable to increase the degree of preferred orientation purposely, so that the powder specimen approximates a two-dimensional crystal as, for example, to suppress certain reflections or to find trace amounts of another phase.

TRANSMISSION SPECIMEN-FOCUSING MONOCHROMATOR

Monochromators normally have been used to obtain monochromatic radiation. It is now possible to use scintillation or proportional counters with pulse-amplitude discrimination (see below) which give low backgrounds and practically the same peak-to-background ratio as Geiger counter diffractometers equipped with monochromators (Parrish and Kohler, 1956a). However, monochromators occasionally are required and their use may supplement the standard equipment. There are several methods for using a monochromator with the diffractometer (see for example, Triplett *et al.*, 1954; Cummings, Kaulitz and Sanderson, 1955; Lang, 1956; Leineweber and Heller, 1957). A curved focusing monochromator crystal rather than a flat nonfocusing crystal is required in order to avoid large intensity losses. There are four possible arrangements with a reflection monochromator: it may be placed either before or after the specimen, and the specimen may be used either in reflection or transmission.

For clay mineral analysis the use of a transmission specimen followed by a focusing reflection monochromator is preferred. This arrangement (Fig. 12) allows comparison of the transmission pattern with a reflection pattern obtained on a standard diffractometer, eliminates the effects of specimen fluorescence, and has certain geometrical advantages which are described below. The intensity loss caused by the monochromator is partially compensated by the use of larger angular apertures so that the intensities are lower by a factor of only 2 compared to the standard diffractometer set up for maximum resolution. In addition, much smaller volumes are required for transmission specimens.

The counter tube arm of the standard diffractometer goniometer must be modified to hold the monochromator, and the counter tube must be moved further out on the arm. The counter tube and specimen rotate in a 2 : 1

https://doi.org/10.1346/CCMN.1958.0070115 Published online by Cambridge University Press

relationship as in the standard instrument. The monochromator is a flat plate of quartz cut at about 3° to the 10·1 planes and elastically bent in a special device so that its surface approximates a section of a logarithmic spiral (de Wolff, Lowitzsch and Parrish, 1956, modified from de Wolff, 1948). The focusing is adjusted by changing the curvature of the crystal. The $K\alpha_1$ and $K\alpha_2$ lines are focused together at some selected diffraction angle, say 30° 2 θ, and the pattern consists of only single lines over a wide angular range up to about 65° 2 θ. This achromatic arrangement is useful in studying line profiles. Unlike the standard diffractometer, the receiving slit does not control the resolution or intensity, as these are determined by the monochromator. The geometrical errors, such as specimen surface displacement, are proportional to sin θ rather than cos θ as is the case in reflection, and hence the method is ideally suited to measuring large *d*-spacings.

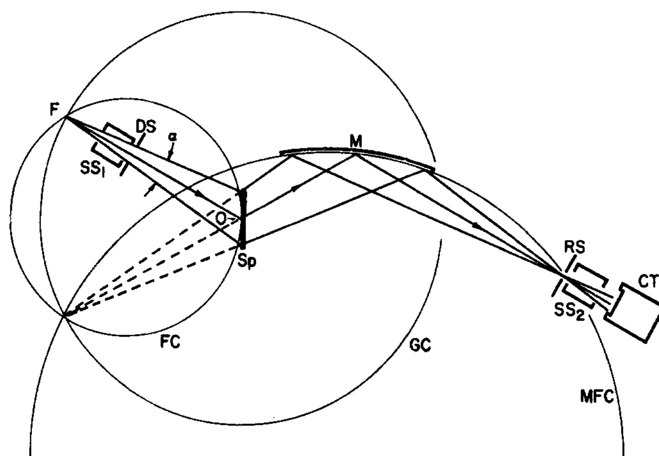

FIGURE 12.—X-ray optical arrangement of diffractometer modified for transmission specimen *Sp* and focusing crystal monochromator *M*. The virtual image of the source is at the focal point of the specimen in reflection as shown by dotted lines; *a*, angular aperture of primary beam, *CT* counter tube, *MFC* monochromator focusing circle; other symbols have same meanings as given in Figs. 2 and 4.

At small diffraction angles the alignment of the reflection instrument is extremely critical and the intensities may be low because small apertures are required, whereas in transmission these problems are less troublesome. It appears that the transmission diffractometer will become an important supplement to the reflection diffractometer.

X-RAY COUNTERS

The use of Geiger counters as X-ray detectors for powder diffractometry became widespread after World War II. Using these detectors, it is possible to make direct, rapid and accurate quantitative measurements of intensities and to record complete line profiles, whereas this could be done only with

https://doi.org/10.1346/CCMN.1958.0070115 Published online by Cambridge University Press

great difficulty using film. The high sensitivity of the counter stimulated the development of improved instrument geometries that had greater precision and resolution and gave better line shapes than could be obtained with film. In fact, the large recent growth of x-ray analysis was the outcome of the development of instruments employing counter tubes, and many of the applications that are now widely used are dependent on counter tube techniques for their success.

The Geiger counter (Friedman, 1949 ; Curtiss, 1950) is the simplest counter tube to use, requires only a minimum of electronic circuitry, is extremely

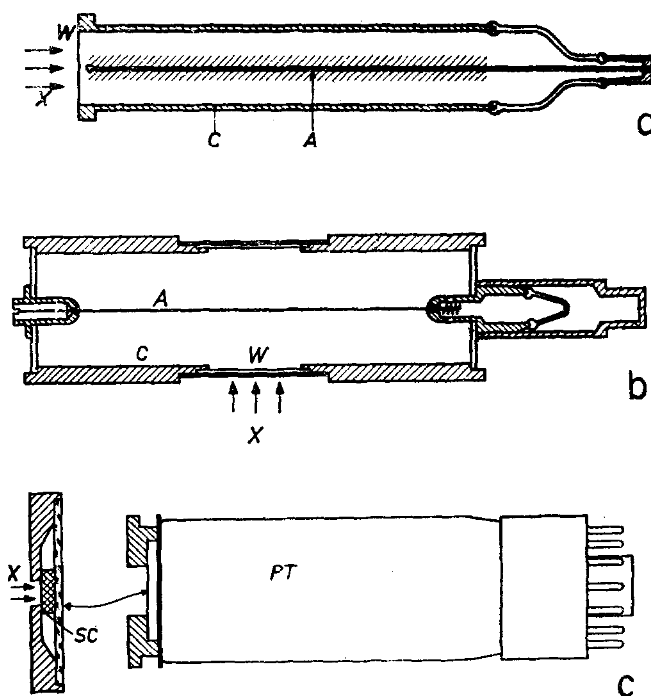

FIGURE 13.—Cross-sections of three important types of x-ray counters. (a) Geiger counter ; (b) proportional counter ; (c) scintillation counter. The arrows X show the direction of the incident x-ray beam, W window, C cathode, A anode, SC scintillation crystal, PT photomultiplier tube. (*Philips Tech. Rev.*, v. 18, 1957).

reliable, and has a very long life. However, it has the disadvantage of a nonlinear response and hence can be used only at relatively low intensities. In the past few years proportional and scintillation counters have been developed for x-ray analysis. Although they require some additional electronic circuitry (high gain linear amplifier), their use eliminates the nonlinearity problem, greatly extends the intensity range, and makes it possible to apply electronic discrimination to achieve lower backgrounds with little loss of peak intensity (Parrish and Kohler, 1956a). Ionization chambers, crystal

https://doi.org/10.1346/CCMN.1958.0070115 Published online by Cambridge University Press

detectors, direct photomultipliers and image intensifier tubes have not proved competitive with the counter tubes mentioned above for the wavelength and intensity range normally used in x-ray analysis, and therefore the discussion will be confined to the three detectors mentioned above and shown in Fig. 13.

In film methods the intensities of all the lines or spots are integrated over a considerable period of time. Counter methods, on the other hand, accumulate data point by point, and hence it is necessary that the primary x-ray tube intensity be well stabilized for short as well as long periods of time in order to obtain significant measurements of the relative intensities.

Properties of Counter Tubes

Three of the more important factors that must be considered in the selection of a counter tube for x-ray analysis are : linearity of response, quantum counting efficiency and the pulse amplitude distribution.

Linearity.—The linearity of the counter system is limited by the resolving time of the counter tube or scaling circuit, whichever is the longer. Geiger counters have a resolving time of the order of 50–300 μsec depending on the geometry, gas filling and voltage of the counter tube, and mode of operation and voltage of the x-ray tube (Parrish, 1959). For example, if a particular counter has a resolving time of 270 μsec for a particular set of conditions and the true counting rates are 500, 1000 and 1500 c/sec, the observed counting rates would be 440, 790 and 1070 c/sec, respectively. The effect of the resolving time on the relative intensities of the lines is illustrated in Table 2. At higher counting rates the counter tube may choke and be useless.

The departure from linearity of the Geiger counter can be checked with monochromatic x-rays reflected from a single crystal plate (using very small apertures) and a number of foils of equal absorption. The counting rate is measured as each foil is inserted in the beam and is plotted on a logarithmic

TABLE 2.—EFFECT OF NONLINEARITY OF GEIGER COUNTERS ON RELATIVE INTENSITIES[1]

	Low Intensity			High Intensity		
hk·l	*P–B* (c/sec)	Peak Ratios	Integr. Ratios	*P–B* (c/sec)	Peak Ratios	Integr. Ratios
10·0	83	25	19	1152	47	30
10·1	332	100	100	2440	100	100
10·2	25	8	7	456	19	13
11·1	16	5	4	253	10	6
20·0	17	5	5	384	16	12
20·1	13	4	3	256	10	6

[1] Quartz powder specimen, CuKα radiation, 40 kVp, 1 mA for low intensity, 20 mA for high intensity, *P–B* measurements with ratemeter, integrated line intensity measurements with scaling circuit, Geiger counter resolving time 270 μsec.

https://doi.org/10.1346/CCMN.1958.0070115 Published online by Cambridge University Press

scale against the number of foils on a linear scale. Although it is a simple matter to correct for nonlinearity of peak readings up to about 1200 c/sec, it is difficult to make corrections for integrated line intensity measurements because the counting rate is continually changing (du Pré, 1953).

Proportional and scintillation counters have resolving times of the order

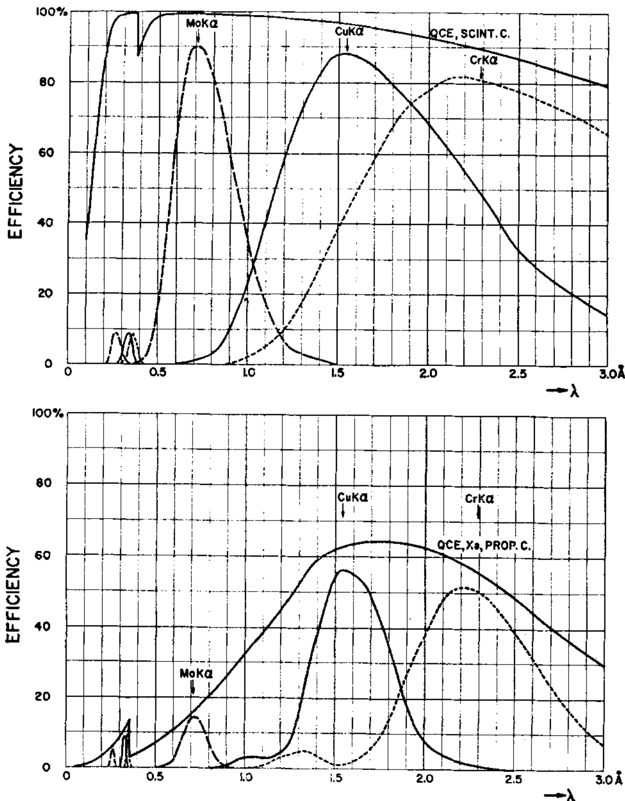

FIGURE 14.—Modification of response of detector system by use of pulse height analyzer. Above, NaI–Tl scintillation counter ; below, xenon proportional counter. The upper solid line shows the quantum counting efficiency *QCE*, and the lower curves show the efficiency of the detector system when the pulse height analyzer is set to pass 90 percent of MoKα, CuKα or CrKα radiation. The small curves on the lower left side are the escape peaks (*Rev. Sci. Instr.*, v. 27, 1956).

of 0.2 μsec and hence are linear up to very high counting rates. With these counters the limitation in linearity is usually the electronic circuits. The scaling circuit may have a resolving time of 1–10 μsec and the pulse height analyzer may be linear up to counting rates of 5000–15,000 c/sec.

Quantum counting efficiency.—The number of x-ray quanta detected compared with the number that strike the counter tube window is dependent

https://doi.org/10.1346/CCMN.1958.0070115 Published online by Cambridge University Press

on the absorption of the window and the absorption of the gas filling of the Geiger and proportional counter or the scintillation crystal (Taylor and Parrish, 1955). This efficiency, usually expressed in percent, varies from one type of counter to another and with the x-ray wave length. The upper solid lines of Fig. 14 show the calculated quantum counting efficiency as a function of wave length for the NaI–Tl scintillation counter and the xenon side-window proportional counter. The efficiency of the argon end-window Geiger counter is nearly the same as that of the proportional counter except for the absence of the sharp increase at the XeK-absorption edge. In these calculations it is assumed that there are no losses due to nonlinearity, and that the counter tube has a uniform radial sensitivity. The latter is true in the case of the scintillation counter but may not be true for Geiger and proportional counters (Van Zoonen, 1955).

In order to obtain the maximum precision in the available counting time, it is desirable to select a counter tube with a high efficiency for the radiation being measured. Thus for the same experimental conditions a scintillation counter will give seven times more counts of MoKα and nearly two times more counts of CuKα than an argon-filled Geiger counter. Consequently the statistical precision will be increased approximately by $7^{\frac{1}{2}}$ and $2^{\frac{1}{2}}$, respectively, in the same counting time.

The spectrum from the x-ray tube contains a large amount of continuous radiation which is scattered by the specimen and recorded as x-ray background. Most of the continuum is of much shorter wave length than the line spectrum. The gas-filled counter tubes have a low efficiency for the short wave-length radiation and hence act as crude monochromators, thereby decreasing the background (Parrish and Hamacher, 1952 ; Parrish and Kohler, 1956b). The scintillation counter, however, has nearly equal sensitivity for all the wave lengths, and hence the x-ray background is considerably higher. The use of electronic discrimination (see below) eliminates most of the background so that the peak-to-background with the scintillation counter is comparable to that obtained with the gas-filled detectors and in addition it has the advantage of a higher quantum counting efficiency.

Pulse amplitude distribution.—One of the important advantages of proportional and scintillation counters over Geiger counters is that the average amplitude A of the pulses produced in the x-ray quantum absorption process is proportional to the energy of the quantum. When monochromatic x-rays (i.e. x-rays of a single energy) are absorbed in these counters, a distribution of pulse amplitudes is obtained, and the width of the distribution W divided by A expresses the energy resolution of the detector. The smaller the ratio W/A, the better the energy resolution. Typical values for CuKα radiation are 20 percent for the proportional counter and 50 percent for the scintillation counter.

By using a single channel pulse-height analyzer it is possible to limit the range of pulse amplitudes passed on to the scaling circuit. The base of the analyzer is set to reject all pulses smaller than a selected amplitude and the window is set to reject those pulses greater than a selected amplitude

https://doi.org/10.1346/CCMN.1958.0070115 Published online by Cambridge University Press

(Parrish and Kohler, 1956a; Dowling *et al.*, 1956–1957; Parrish, 1959). This is illustrated in Fig. 15 which shows the pulse amplitude distribution for CuKα radiation obtained with the scintillation counter. These distributions may be recorded with the analyzer window set at about 1 V and the base-level driven downward at a constant rate starting at, say, 40 V. The average pulse amplitude can be increased or decreased by changing the counter tube voltage or gain of the amplifier, or both. It should be high enough so that the tail on the low pulse height side is removed from the counter tube noise, which may begin to appear at about 5 V, but not too high, so that the entire distribution can fit into the window width.

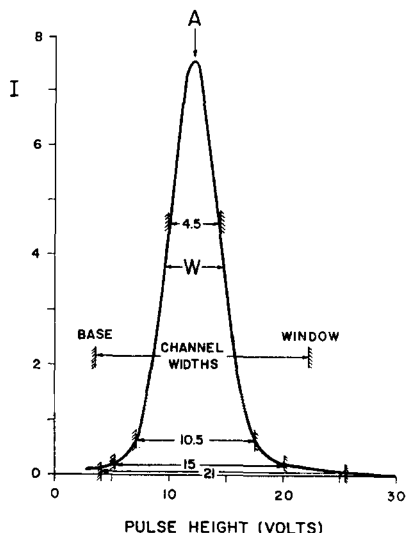

FIGURE 15.—The pulse amplitude distribution of the scintillation counter with monochromatic CuKα radiation. The base (*left*) and window (*right*) settings of the pulse height analyzer are those used in Table 3.

Detailed studies of the spectral distribution of the recorded background obtained with the discrimination method on powder samples show that it usually is unwise to cut off more than 5 percent of the distribution with the base and 5 percent with the window. If more than 10 percent is cut off, the peak intensity drops faster than the peak-to-background ratio increases, as shown in Table 3 for the same settings given in Fig. 15. In addition, settings on the steep slope of the distribution require extraordinary stability from the circuits to avoid serious variations in intensity. The curves below the quantum efficiency curves in Fig. 14 show the variation in efficiency of the counter system when the pulse height analyzer is set to pass 90 percent of MoKα, CuKα and CrKα using a proportional and scintillation counter. The x-ray background from powder samples that remains after discrimination contains at least as much (and usually considerably more) characteristic radiation as noncharacteristic radiation. The peak-to-background ratios for non-

https://doi.org/10.1346/CCMN.1958.0070115 Published online by Cambridge University Press

TABLE 3.—EFFECT OF PULSE HEIGHT ANALYZER WINDOW[1]

Base	Channel Width	*P–B*	*B*	(*P–B*)/*B*	Non-x-ray
4	21	2720	320	9	5
5	15	2683	37	73	1
7	10.5	2558	32	80	—
10	4.5	1679	19	88	—

[1] Cu target, 40 kVp, 16 mA, 0.0007 in. Ni filter, α 0.5°, receiving slit 0.05°, scintillation counter, dickite (7 Å), St. George, Utah. Background measured at 13° 2θ, base and window settings in volts, *P–B*, *B* and non x-ray background in counts/sec. The pulse height analyzer settings are shown in Fig. 15.

fluorescent specimens are thus about the same as those obtained with efficient monochromator systems.

Other factors.—Two or more pulse amplitude distributions may occur even when monochromatic radiation is employed. These secondary distributions, called " escape peaks," arise when the incident x-rays cause the gas or scintillation crystal to fluoresce and the fluorescent radiation escapes from the active volume of the counter (Parrish and Kohler, 1956a). Escape peaks (Fig. 14) may have a significant influence on the efficiency when the pulse height analyzer is used. With MoKα radiation and a krypton-filled proportional counter, more than one-half the pulses occur in the escape peak, and when the base-level setting of the analyzer is set to reject the escape peak, the efficiency decreases by more than a factor of 2. Fortunately this phenomenon is not common in the detector systems used for x-ray analysis.

The discrimination method is also useful in reducing the non-x-ray background. Tube noise, cosmic rays and radioactivity all contribute to the background, and may become troublesome when measuring weak intensities. The scintillation counter equipped with a small volume scintillation crystal is particularly useful for measuring radioactive samples (Kohler and Parrish, 1955).

The placing of the β-filter either between the source and specimen or between specimen and counter tube may also exert a considerable effect on the peak-to-background ratio. In some instances one position is better than the other (Parrish and Taylor, 1956). It sometimes is not realized that specimen fluorescence is often caused by the continuous radiation as well as the line spectrum. In such cases it is desirable to select a target whose β-filter nearly completely absorbs the specimen fluorescence and transmits the Kα line. For example, in the case of a Cu target and a Cu specimen, the continuum causes a large amount of CuK fluorescence. The Ni filter has a large absorption only for CuKβ and reduces CuKα by only a factor of about 2. Hence the background is high and cannot be reduced with discrimination because it obviously is impossible to discriminate against the same wave length that is to be measured. If a Co target is used instead, the Fe filter will almost completely absorb the CuK fluorescence (as well as the CoKβ)

https://doi.org/10.1346/CCMN.1958.0070115 Published online by Cambridge University Press

and transmit the CoKα, thereby giving a low background. Proper consideration of the absorption and fluorescence thus can lead to considerable improvement of the peak-to-background ratio, and a series of different filters is a useful supplement to the discrimination method.

COUNTING STATISTICS

When using counter tubes it is necessary to take into account the statistical factors associated with the various counting methods (Parrish, 1955–1956a). Even if the average x-ray intensity does not vary during the measurement, two or more successive readings will not necessarily be the same because

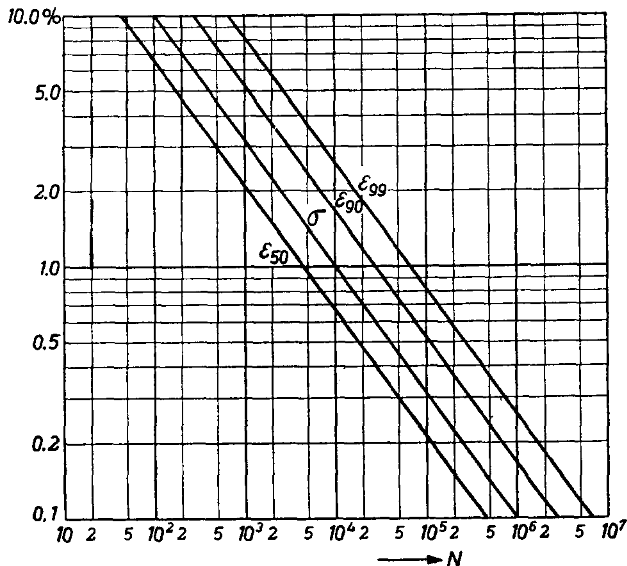

FIGURE 16.—The percentage error as a function of the total number of counts N for various confidence levels ε ; σ = standard deviation (*Philips Tech. Rev.*, v. 17, 1956).

of the random rate at which the quanta reach the counter tube. In theory there is no limit to the precision that can be attained if enough counts are accumulated. In practice the counting time is limited and the x-ray tube intensity does vary by small amounts. To obtain the maximum precision in the minimum counting time and to evaluate the precision of a measurement, it is necessary to give some thought to the selection of the counting method.

Consider an x-ray source in which the variation of intensity with time is very small compared to the precision required in the intensity measurement and let a total number of counts N be accumulated in a certain time interval t. If a very large number of measurements of N are made, the spread of the individual measurements will be given by a Gaussian distribution with a standard deviation $\sigma = \bar{N}^{\frac{1}{2}}$ where $\bar{N}$ is the average value. The relative error

https://doi.org/10.1346/CCMN.1958.0070115 Published online by Cambridge University Press

in any individual measurement is $\epsilon = Q/N^{\frac{1}{2}}$, where Q is a constant determined by the confidence level. Fig. 16 is a plot showing the percentage error as a function of N for the 50, 67 ($Q = 1$, standard deviation σ), 90 and 99 percent confidence levels. It is apparent that a large number of counts must be accumulated to obtain a small percentage error at a high confidence level.

The counting rate $n = N/t$ is usually expressed in counts per second. The background counting rate n_2 must be subtracted from the peak counting rate n_1 (peak + background) to obtain the net peak intensity $n_1 - n_2$. If ϵ_1 and ϵ_2 are the relative errors of n_1 and n_2, respectively, the absolute errors are $n_1\,\epsilon_1$ and $n_2\,\epsilon_2$ and the relative error of the difference is

$$\epsilon_d = \frac{[(n_1\,\epsilon_1)^2 + (n_2\,\epsilon_2)^2]^{\frac{1}{2}}}{n_1 - n_2}$$

The absolute errors of both the peak and background measurements thus have the same influence on ϵ_d. The peak-to-background ratio, particularly when it is small (say < 5), may have a large effect on the precision of the measurement. The optimum apportionment of a given counting time to obtain the maximum precision of the difference or ratio of counting rates may be easily computed (Mack and Spielberg, 1958).

The several methods of measuring intensities with counter tubes may be separated conveniently into two major categories: fixed time and fixed count methods. In the fixed time method the counting time t is constant and the precision of the measurement depends on n. In the fixed count method N is preselected and the precision is the same for all measurements regardless of n. Of course, the amount of time to accumulate N varies with n, and t becomes very long at low counting rates.

To measure a complete line profile, both the fixed time and fixed count methods require point-by-point settings, and the number of points that are measured depends upon the detailed information that is required. Automatic methods are frequently used to facilitate the measurements. A step-gear may be used on the goniometer to scan the line profile at fixed angular increments and the ratemeter output fed to a strip-chart recorder. The recording then has a steplike appearance, and the width of the steps is determined by the recycling time of the step-gear and the chart speed. The same procedure may be used with the fixed count method, and an automatic counting rate computer has been developed for this purpose (Hamacher and Lowitzsch, 1955–1956).

The most common and useful automatic scanning method is to drive the goniometer at a constant angular velocity and record the ratemeter output. This introduces another factor that may reduce the precision of the analysis. This factor is determined by the product of the time constant of the ratemeter circuit and the goniometer scanning speed. Fig. 17 is a series of recordings showing the effect of increasing this product. The recordings show the 12·1 reflection of quartz, which is a partially resolved $CuK\alpha_{1,2}$ doublet scanned from high to low angles and then reversed. When the

https://doi.org/10.1346/CCMN.1958.0070115 Published online by Cambridge University Press

product is small, say 1 sec × deg/min, there is only a small distortion of the line profile, as shown by the fact that both halves of the recording (Fig. 17a) have nearly identical shapes and intensities. The recording in Fig. 17(b) was made at twice the scanning speed and one-half the time constant, and thus has the same product; hence the line shapes are the same as in Fig. 17(a), but the total number of counts accumulated in the recording is only

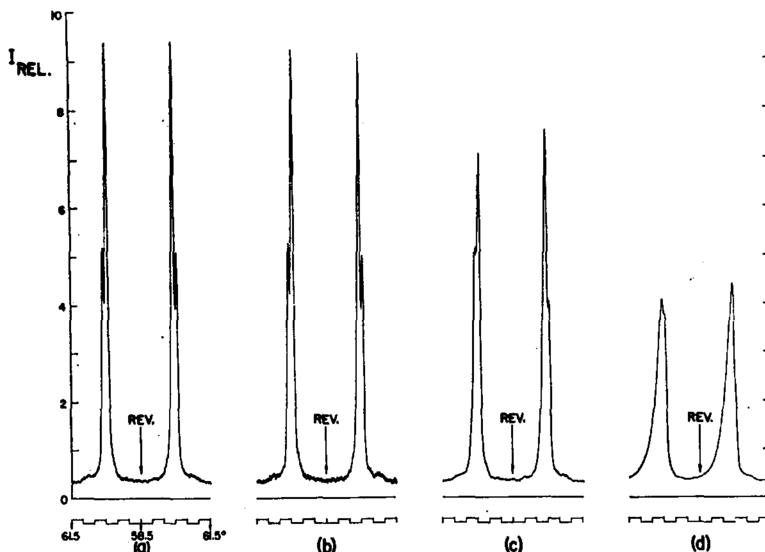

FIGURE 17.—Effect of increasing the time constant and scanning speed on ratemeter recording. $CuK\alpha_{1,2}$, quartz 12·1 reflection, $\alpha = 2°$, receiving slit 0.05°, scintillation counter. Direction of scanning reversed at 58.5° 2θ.

	(a)	(b)	(c)	(d)
Scan Speed (°/min)	¼	½	½	1
Time Constant (sec)	4	2	8	16
Product (sec × °/min)	1	1	4	16
Chart Speed (in./hr)	7½	7½	15	30

one-half as large. When the product is increased to 4 sec × deg/min, as in Fig. 17(c), the distortion is considerable; and when the product reaches 16 the distortion is so great that the $K\alpha_2$ line is higher than the $K\alpha_1$ line.

It is clear from the examples described that increasing the time constant and/or scanning speed decreases the peak intensity, shifts the line in the scanning direction, and asymmetrically broadens the line. The real shape of the line also determines the amount of distortion, and since the $K\alpha$ doublet separation varies with Bragg angle, the amount of distortion is also Bragg angle dependent. Although it is possible to make some corrections for these distortions (Parrish, 1955–1956a; Tournarie, 1954), these are known only approximately.

https://doi.org/10.1346/CCMN.1958.0070115 Published online by Cambridge University Press

The percentage reduction of the peak intensities obtained when scanning in the same direction is the same for all lines regardless of their true intensities (within the limits set by the nonlinearity of the detector system). It was found, for example, that the relative intensities of the front-reflection lines from a quartz powder sample were unchanged even when the time constant $\times$ scanning speed product was increased from 1 to 16, all other experimental conditions remaining unchanged. Hence for routine work requiring only the measurement of relative peak intensities, higher scanning speeds may be safely used provided, of course, that only the values from a particular set of conditions are used.

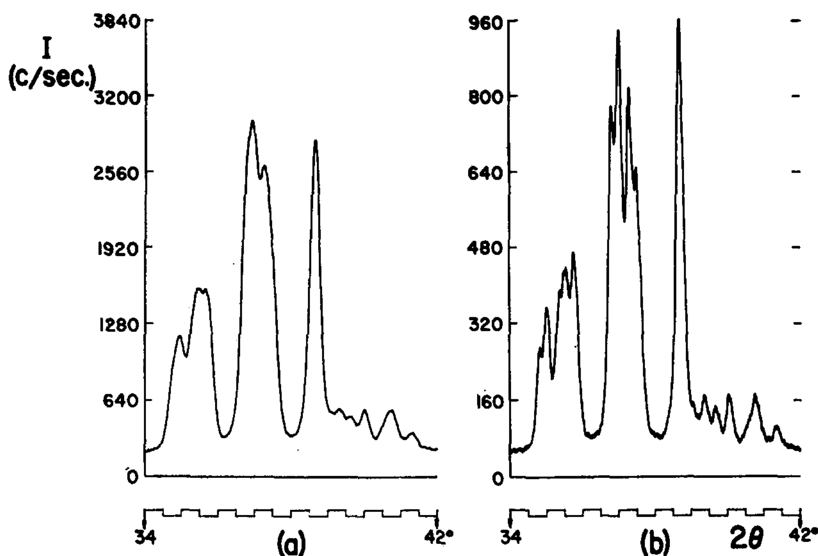

FIGURE 18.—Recordings of a portion of the dickite pattern.

	(a)	(b)
Scan Speed (°/min.)	1	$\frac{1}{4}$
Time Constant (sec)	4	4
Product (sec × °/min.)	4	1
Chart Speed (in./hr)	30	$7\frac{1}{2}$
Receiving Slip (°2θ)	0.20	0.05

Fig. 18 shows two recordings of a portion of the dickite pattern which illustrates some of the points mentioned above. Fig. 18(a) was obtained with 1°/min scan speed, 2 sec time constant and 0.20° receiving slit, and Fig. 18(b) with $\frac{1}{4}$°/min, 4 sec time constant and 0.05° receiving slit. The total number of counts in both recordings thus was the same, but the slower scan with narrow receiving slit provides much more information; lines that appear as one or two components under the rapid scan are seen to consist of several components under better chosen conditions.

https://doi.org/10.1346/CCMN.1958.0070115 Published online by Cambridge University Press

REFERENCES

Alexander, L., Klug, H. P. and Kummer, E. (1948) Statistical factors affecting the intensity of x-rays diffracted by crystalline powders: *J. Appl. Phys.*, v. 19, pp. 742–753.

Brindley, G. W. (Editor) (1951) *X-Ray Identification and Crystal Structures of Clay Minerals*: Mineralogical Society, London, 345 pp.

Buerger, M. J. and Kennedy, G. C. (1958) An improved specimen holder for the focusing-type x-ray spectrometer: *Amer. Min.*, v. 43, pp. 756–757.

Cummings, W. V., Jr., Kaulitz, D. C. and Sanderson, M. J. (1955) Double diffracting x-ray spectrometer for study of irradiated materials: *Rev. Sci. Instr.*, v. 26, pp. 5–13.

Curtiss, L. F. (1950) The Geiger-Müller counter: *Nat. Bur. Stand. Circ.* 490.

deWolff, P. M. (1948) An adjustable curved crystal monochromator for x-ray diffraction analysis: *Appl. Sci. Res.*, B, v. 1, pp. 119–126; Multiple Guinier cameras: *Acta Cryst.*, v. 1, pp. 207–211.

de Wolff, P. M. (1957) Self-centering combined aperture- and scatter-slit for powder diffractometry with constant effective specimen area: *Appl. Sci. Res.*, B, v. 6, pp. 296–300.

de Wolff, P. M., Lowitzsch, K. and Parrish, W. (1956) Application of focusing monochromators to x-ray diffractometry: *Int. Union of Cryst., Madrid.* In preparation.

de Wolff, P. M., Taylor, J. M. and Parrish, W. (1959) Experimental study of effect of crystallite size statistics on x-ray diffractometer intensities: *J. Appl. Phys.*, v. 30, pp. 63–69.

Dowling, P. H., Hendee, C. F., Kohler, T. R. and Parrish, W. (1956–1957) Counter tubes for x-ray analysis: *Philips Tech. Rev.*, v. 18, pp. 262–275.

du Pré, F. K. (1953) The counting loss of a Geiger counter with periodic arrival rate of quanta: *Philips Res. Rpts.*, v. 8, pp. 411–418.

Flörke, O. W. and Saalfeld, H. (1955) Ein Verfahren zur Herstellung texturfreier Röntgen-Pulverpräparate: *Z. Krist.*, v. 106, pp. 460–466.

Friedman, H. (1945) Geiger counter spectrometer for industrial research: *Electronics*, v. 18, pp. 132–137.

Friedman, H. (1949) Geiger counter tubes: *Proc. Inst. Radio Engrs., N.Y.*, v. 37, pp. 791–808.

Hamacher, E. A. and Lowitzsch, K. (1955–56) The " Norelco " counting rate computer: *Philips Tech. Rev.*, v. 17, pp. 249–254.

Keating, D. T. and Warren, B. E. (1952) The effect of low absorption coefficient on x-ray spectrometer measurements: *Rev. Sci. Instr.*, v. 23, pp. 519–522.

Kerr, P. F. *et al.* (1950) Analytical data on reference clay materials: *Amer. Pet. Inst. Project* 49, Prelim. Rept. No. 7.

Kohler, T. R. and Parrish, W. (1955) x-Ray diffractometry of radioactive samples: *Rev. Sci. Instr.*, v. 26, pp. 374–379.

Ladell, J., Parrish, W. and Taylor, J. (1959) Center-of-gravity method of precision lattice parameter determination: *Acta Cryst.*, v. 12, pp. 253–254; Interpretation of diffractometer line profiles: *Ibid, in press.*

Lang, A. R. (1956) Diffracted-beam monochromatization techniques in x-ray diffractometry: *Rev. Sci. Instr.*, v. 27, pp. 17–25.

Leineweber, G. and Heller, E. (1957) Zur Intensitätsmessung von Röntgeninterferenzen. II. Zählrohrgoniometermessungen an Pulverpräparaten mit Hilfe von kristallreflektierter monochromatisher Strahlung: *Z. Krist.*, v. 109, pp. 198–203.

Lindemann, R. and Trost, A. (1940) Das Interferenz-Zählrohr als Hilfsmittel der Feinstrukturforschung mit Röntgenstrahlen: *Z. Phys.*, v. 115, pp. 456–468.

Mack, M. (1956) Bibliography of x-ray spectrochemical analysis: fluorescence and absorption: *Norelco Reptr.*, v. 3, pp. 37–39.

Mack, M. and Spielberg, N. (1958) Statistical factors in x-ray intensity measurements: *Spectrochim. Acta*, v. 12, pp. 169–178.

McCreery, G. L. (1949) Improved mount for powdered specimens used on the Geiger-counter x-ray spectrometer: *J. Amer. Ceram. Soc.*, v. 32, pp. 141–146.

https://doi.org/10.1346/CCMN.1958.0070115 Published online by Cambridge University Press

Milberg, M. E. (1958) Transparency factor for weakly absorbing samples in x-ray diffractometry : *J. Appl. Phys.*, v. 29, pp. 64–65.

Parrish, W. (1949) x-Ray powder diffraction analysis : film and Geiger counter techniques : *Science*, v. 110, pp. 368–371.

Parrish, W. (1955–1956a) x-Ray intensity measurements with counter tubes : *Philips Tech. Rev.*, v. 17, pp. 206–221.

Parrish, W. (1955–1956b) x-Ray spectrochemical analysis : *Philips Tech. Rev.*, v. 17, pp. 269–286.

Parrish, W. (1958) Optimum x-ray tube focal spot geometry for powder diffractometry : *Am. Cryst. Assoc., Milwaukee Meeting*, Paper G–8, p. 35.

Parrish, W. (1959) Geiger, proportional and scintillation counters : *Int. Tables for X-ray Cryst.*, v. 3. In press.

Parrish, W. and Hamacher, E. A. (1952) Geiger counter x-ray spectrometer ; instrumentation and techniques : *Trans. Instr. and Meas. Conf., Stockholm*, pp. 95–105.

Parrish, W., Hamacher, E. A. and Lowitzsch, K. (1954–1955) The " Norelco " x-ray diffractometer : *Philips Tech. Rev.*, v. 16, pp. 123–133.

Parrish, W. and Kohler, T. R. (1956a) The use of counter-tubes in x-ray analysis : *Rev. Sci. Instr.*, v. 27, pp. 795–808.

Parrish, W. and Kohler, T. R. (1956b) A comparison of x-ray wavelengths for powder diffractometry : *J. Appl. Phys.*, v. 27, pp. 1215–1218.

Parrish, W. and Lowitzsch, K. (1959) Geometry, alignment and angular calibration of x-ray diffractometers : *Amer. Min.*, v, pp. 765–787.

Parrish, W. and Taylor, J. (1956) Beta filters for x-ray diffractometry : *Norelco Reptr.*, v. 3, pp. 105–106.

Parrish, W. and Wilson, A. J. C. (1959) Precision measurement of lattice parameters of polycrystalline specimens : *Int. Tables for X-ray Cryst.*, v. 2, pp. 216–234.

Pike, E. R. (1957) Counter diffractometer—the effect of vertical divergence on the displacement and breadth of powder diffraction lines : *J. Sci. Instr.*, v. 34, pp. 355–363 ; (1959) *Ibid.*, v. 36, pp. 52–53.

Pike, E. R. and Wilson, A. J. C. (1959) Counter diffractometer—the theory of the use of centroids of diffraction profiles for high accuracy in the measurement of diffraction angles : *Brit. J. Appl. Phys.*, v. 10, pp. 57–71.

Porrenga, D. H. (1958) The application of a multiple Guinier camera (after P. M. de Wolff) in clay mineral studies : *Amer. Min.*, v. 43, pp. 770–774.

Smallman, C. R. (1952) A sample holder for the Norelco high angle goniometer : *Rev. Sci. Instr.*, v. 23, pp. 135–136.

Taylor, J. and Parrish, W. (1955) Absorption and counting efficiency data for x-ray detectors : *Rev. Sci. Instr.*, v. 26, pp. 367–373 ; *Ibid.*, v. 27, p. 108.

Tournarie, M. (1954) Correction de l'erreur systématique due à l'enregistrement continu au spectromètre à rayon x : *J. Phys. Radium*, Suppl. no. 1, v. 15, pp. 16A–22A.

Triplett, W. B., Hauser, J. J., Wells, C. and Mehl, R. F. (1954) Determination of retained austenite by a Geiger counter x-ray technique : *Wright Air Development Center Tech. Rpt.* 53–518.

Van Zoonen, D. (1955) The efficiency of halogen-quenched Geiger-counters for x-rays : *Appl. Sci. Res.*, v. 4, pp. 196–204.

Warren, B. E. (1959) x-Ray studies of deformed metals: *Progress in Metal Physics*, v. 8, Pergamon Press Ltd., London.

Wilson, A. J. C. (1949) *X-Ray Optics* : Methuen, London.

Wilson, A. J. C. (1950) Geiger counter x-ray spectrometer—influence of size and absorption coefficient of specimen on position and shape of powder diffraction maxima : *J. Sci. Instr.*, v. 27, pp. 321–325.

https://doi.org/10.1346/CCMN.1958.0070115 Published online by Cambridge University Press